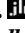


Dysosmobacter welbionis effects on glucose, lipid, and energy metabolism are associated with specific bioactive lipids

Emilie Moens de Hase^{1,2} , Camille Petitfils³, Mireille Alhouayek⁴ , Clara Depommier^{1,2},
Pauline Le Faouder⁵, Nathalie M. Delzenne¹ , Matthias Van Hul^{1,2} , Giulio G. Muccioli^{4,‡} ,
Nicolas Cenac^{3,‡} , and Patrice D. Cani^{1,2,6,*} 

¹Metabolism and Nutrition Research group, Louvain Drug Research Institute (LDRI), UCLouvain, Université catholique de Louvain, Brussels, Belgium; ²WELBIO-Walloon Excellence in Life Sciences and Biotechnology, WELBIO department, WEL Research Institute, Wavre, Belgium; ³IRSD, INSERM, INRA, INP-ENVT, Toulouse University 3 Paul Sabatier, Toulouse, France; ⁴Bioanalysis and Pharmacology of Bioactive Lipids Research Group (BPBL), Louvain Drug Research Institute (LDRI), UCLouvain, Université catholique de Louvain, Brussels, Belgium; ⁵MetaToulLipidomics Facility, INSERM UMR1048, Toulouse, France; ⁶Institute of Experimental and Clinical Research (IREC), UCLouvain, Université catholique de Louvain, Brussels, Belgium

Abstract The newly identified bacterium *Dysosmobacter welbionis* J115^T improves host metabolism in high-fat diet (HFD)-fed mice. To investigate mechanisms, we used targeted lipidomics to identify and quantify bioactive lipids produced by the bacterium in the culture medium, the colon, the brown adipose tissue (BAT), and the blood of mice. In vitro, we compared the bioactive lipids produced by *D. welbionis* J115^T versus the probiotic strain *Escherichia coli* Nissle 1917. *D. welbionis* J115^T administration reduced body weight, fat mass gain, and improved glucose tolerance and insulin resistance in HFD-fed mice. In vitro, 19 bioactive lipids were highly produced by *D. welbionis* J115^T as compared to *Escherichia coli* Nissle 1917. In the plasma, 13 lipids were significantly changed by the bacteria. C18-3OH was highly present at the level of the bacteria, but decreased by HFD treatment in the plasma and normalized in *D. welbionis* J115^T-treated mice. The metabolic effects were associated with a lower whitening of the BAT. In the BAT, HFD decreased the 15-deoxy- $\Delta^{12,14}$ -prostaglandin J₂, a peroxisome proliferator-activated receptor (PPAR- γ) agonist increased by 700% in treated mice as compared to HFD-fed mice. Several genes controlled by PPAR- γ were upregulated in the BAT. In the colon, HFD-fed mice had a 60% decrease of resolvin D5, whereas *D. welbionis* J115^T-treated mice exhibited a 660% increase as compared to HFD-fed mice.  In a preliminary experiment, we found that *D. welbionis* J115^T improves colitis. In conclusion, *D. welbionis* J115^T influences host metabolism together with several bioactive lipids known as PPAR- γ agonists.

Supplementary key words *Dysosmobacter welbionis* J115^T • obesity • bioactive lipids • brown adipose tissue • colon • dietary fat • glucose • insulin resistance • inflammation • lipidomics

The obesity epidemic continues to increase globally. In this context, unraveling novel mechanisms and biological systems involved in obesity etiology is highly pertinent. Among the potential targets, the gut microbiota is viewed as an important factor impacting host physiology (1). Numerous observational studies are showing different associations between gut microbiota composition and/or functionality and host diseases (2). However, demonstrating causation for specific taxa remains difficult (3). Over the last decade, potential next generation beneficial bacteria have been identified. Among those, the symbiont *Akkermansia muciniphila* has been extensively studied in preclinical research and identified as a potential new target to tackle metabolic disorders and related diseases (4). Among the mechanisms, it has been shown that *A. muciniphila* produces short-chain fatty acids, such as propionate and thereby contributes to host health (5). Besides the well-described effects of short-chain fatty acids on host health, recent evidence suggests that other mechanisms might be involved in the effects of some probiotic bacteria. For instance, it has also been shown that this bacterium produces different types of proteins (e.g., P9 and Amuc_1100) that are acting on immune receptors and partially explaining the beneficial effects (6, 7) (for review (4)). Recently, two independent studies have shown that specific bioactive lipids might also be involved. In fact, the administration of *A. muciniphila* in both mice and humans increases colonic tissue or blood levels of 1-palmitoyl-glycerol and 2-palmitoyl-glycerol, two endocannabinoid-related lipids that are endogenous activators of peroxisome

[‡]These authors contributed equally to this work.

*For correspondence: Patrice D. Cani, patrice.cani@uclouvain.be.

proliferator-activated receptor alpha (PPAR- α) (8, 9). Another study shows that a phosphatidylethanolamine with two branched chains (a15:0-i15:0 PE) isolated from the membrane of *A. muciniphila* had immunogenic activity by acting through toll-like receptor TLR2-TLR1 heterodimer (10).

Escherichia coli Nissle 1917 (EcN) is another beneficial bacterium that can be used as treatment for inflammatory bowel diseases (11). Recently, we contributed to the discovery of a novel anti-inflammatory mechanism of EcN (11). By using large-scale lipidomic, we found that a bacterial long-chain fatty acid hydroxylated on the third carbon, C18-3OH, could reduce colitis in mice by activating PPAR- γ into the intestinal epithelial cells (11).

We have recently isolated and described a novel bacterium, named *Dysosmobacter welbionis* J115^T (12). This bacterium is prevalent and abundant in the general healthy population and found to be lower in type 2 diabetic subjects and to correlate negatively with BMI, fasting glucose and glycated hemoglobin (13). In mice, we found that supplementation with *D. welbionis* J115^T reduces diet-induced obesity, glucose intolerance, and brown adipose tissue (BAT) inflammation in association with an increased mitochondria amount and non-shivering thermogenesis (13). Although *D. welbionis* J115^T has been identified as a butyrate producer, we were unable to find a higher butyrate content in feces or in the blood of treated mice. Therefore, as for other bacteria such as *A. muciniphila* or EcN, we investigated whether *D. welbionis* J115^T could produce specific bioactive lipids in the culture medium. These results were compared with lipids produced by EcN as this known probiotic has been studied for its production of bioactive lipids. We also studied whether the beneficial effects observed were linked with changes in the abundance of different bioactive lipids within the BAT, the colon, and the blood of high-fat diet (HFD)-fed mice treated with *D. welbionis* J115^T.

MATERIAL AND METHODS

Culture and preparation of *Dysosmobacter welbionis* for mice experiments

D. welbionis J115^T was cultured anaerobically in a modified yeast casitone fatty acid medium supplemented with 10 g/l inositol. Cultures were centrifuged at 5000 *g* during 15 min, and the supernatant was removed. Cells were then resuspended in anaerobic PBS-carbonate buffer supplemented with 15% (vol/vol) trehalose then immediately frozen in anaerobic vials and stored at -80°C . The number of total and cultivable bacteria administered to the mice was calculated by plating the bacterial culture before preparation and the bacterial suspension after preparation for mice administration.

Mice experiment

HFD experiment. Sets of 7-week-old C57BL/6J male mice (Janvier Laboratories, Le Genest-Saint-Isle, France) were housed in pairs in specific opportunistic and pathogen-free

conditions and in a controlled environment (room temperature of $22 \pm 2^{\circ}\text{C}$, 12 h daylight cycle) with free access to sterile food (irradiated) and sterile water. Upon arrival, all mice underwent a 1-week acclimatization period, during which they were fed a control diet (AIN93Mi, Research Diet, New Brunswick, NJ). During the experiments, food and water intake were recorded once a week. Body composition was assessed by using a 7.5 MHz time domain-NMR (LF50 minispec, Bruker, Rheinstetten, Germany).

The purpose of this mice experiment was to confirm the previously described impact of a daily administration of frozen *D. welbionis* J115^T on diet-induced obesity. A set of 30 mice was divided in three groups of 10 mice. The mice were fed a control diet (AIN93Mi; Research diet, New Brunswick, NJ) or a HFD (60% fat and 20% carbohydrates (kcal/100g), D12492, Research diet, New Brunswick, NJ). One group of HFD-fed mice was treated with an oral administration of *Dysosmobacter welbionis* J115^T by oral gavage at the dose 1.0×10^9 cfu /0.2 ml per day and per mice (HFD + J115), and control groups were treated with an oral gavage of an equivalent volume of PBS-carbonate buffer supplemented with 15% (weight/vol) trehalose (HFD). Treatment continued for 10 weeks. Mice were euthanized after a 6-h fasting period.

All mouse experiments were approved by the board of the Ethical Committee for Animal Care of the Health Sector of the Université Catholique de Louvain (UCLouvain) headed by Prof. J-P Dehoux, under number 2017/UCL/MD/005, and were performed in accordance with the guidelines of the Local Ethics Committee and in accordance with the Belgian Law of 29 May 2013, regarding the protection of laboratory animals (agreement number LA1230314).

Dextran sulfate sodium experiment. Male C57BL/6 mice (8 weeks of age) were obtained from Janvier Labs (Le Genest-Saint-Isle, France), housed in standard filter-top cages, and provided food and drinking water ad libitum. Animals were kept in a controlled environment (room temperature of $22 \pm 2^{\circ}\text{C}$, 12 h daylight cycle) with free access to sterile food (irradiated) and sterile water. Starting at day 0, mice were treated with an oral administration of *Dysosmobacter welbionis* J115^T by oral gavage at the dose 1.0×10^9 cfu /0.2 ml per day and per mice (DSS + J115) and control groups were treated with an oral gavage of an equivalent volume of PBS-carbonate buffer supplemented with 15% (weight/vol) trehalose (Vehicle). To induce colitis, 5% DSS was added to the drinking water over a 5-day period starting at day 7, and this solution was replaced with normal drinking water for an additional 2 days (14). Mice ($n = 9$ per group) were euthanized on day 14 under isoflurane anesthesia.

Oral glucose tolerance test

One week before the end of experiment, the mice were fasted for 6 h before being given an oral gavage glucose load (2 g glucose per kg body weight). Blood glucose was measured 30 min before (time point -30), just prior the oral glucose load (time point 0) and then after 15, 30, 60, 90, and 120 min. Blood glucose was determined with a glucose meter (Accu Check, Roche, Switzerland) on blood samples collected from the tip of the tail vein. Plasma insulin concentration was determined using an ELISA kit (Mercodia, Uppsala, Sweden) according to the manufacturer's instructions.

Tissue sampling

The animals were anesthetized with isoflurane (Forene®, Abbott, Queenborough, Kent, England), and blood was

collected from the portal and cava veins. Then mice were immediately euthanized by cervical dislocation. Tissue samples (liver, BAT, subcutaneous adipose tissue (AT), mesenteric AT, jejunum, ileum and proximal colon, muscles, and brain) were dissected, immersed in liquid nitrogen, and stored at -80°C for further analysis. A part of the ATs and intestines was fixed in 4% paraformaldehyde in PBS for histological analysis.

For the DSS experiment, tissues were removed at the time of death and snap frozen in liquid nitrogen for myeloperoxidase (MPO) activity and ELISA. Before freezing, colons were examined for gross macroscopic appearance, and their weight and length were recorded.

Histological analyses

BAT depots were fixed in 4% paraformaldehyde for 24 h at room temperature. Samples were then dehydrated by immersion in ethanol 100% for 24 h and processed for paraffin embedding. Paraffin sections of 5 μm were stained with haematoxylin and eosin. Whole tissue sections were digitized using a Pannoramic ScanII slide scanner (3DHISTECH) with a 20 \times Plan-Apochromat objective and visualized with Cytomine web platform. White area in BAT corresponds to the lipid droplets and was quantified from five fields per sample using Fiji software.

Lipid analysis

Total FA profiling. Bacterial pellets were extracted in 2.5 ml of methanol (MeOH), 2% acetic acid, 2 ml of water, and 2.5 ml of CH_2Cl_2 . Samples were centrifuged 6 min at 2500 rpm, and the bottom phase was put into new tubes for hydrolyzation. The lipid extract was hydrolyzed in KOH (0.5 M in methanol) at 55°C for 30 min and transmethylated in 1 ml of BF₃-methanol and 1 ml of heptane at 80°C for 1 h. After the addition of 1 ml H₂O to the crude, FAs methyl esters extract was extracted with 2 ml of heptane, dried, and dissolved in 20 μl of EtOAc. One microliter of FAs methyl esters extract was analyzed by GC on a Clarus 600 PerkinElmer system using a FameWax RESTEK fused silica capillary column (30 m \times 0.32 mm, 0.25 μm film thickness). Oven temperature was programmed from 110°C to 220°C at a rate of $2^{\circ}\text{C}/\text{min}$ and the carrier gas was hydrogen (0.5 bar). The injector and the detector temperatures were at 225°C and 245°C , respectively. All of the quantitative calculations were based on the chromatographic peak area relative to the internal standards (ISs).

Free fatty acid metabolites profiling. Bioactive lipids were quantified from bacteria, mouse colons, bloods, and BAT by MS after lipid extraction as previously described (15). After the addition of 500 μl of PBS, and 5 μl deuterated IS mixture (5-HETEd8, LxA4d4, and LtB4d4), the colons were crushed in lysing MatrixA tubes in a precellys (Bertin Technologies). After two crush cycles (6.5 ms–1, 30 s), 10 μl of suspensions were withdrawn for protein quantification and 0.3 ml of cold MeOH were added. The samples were centrifuged at 1016 g for 15 min (4°C), and the resulting supernatants were submitted to solid-phase extraction of lipids using hydrophilic-lipophilic-balanced plate (OASIS® hydrophilic-lipophilic-balanced 30 mg, 96-well plate, Waters, Saint-Quentin-en-Yvelines, France). Briefly, plates were conditioned with 500 μl MeOH and 500 μl H₂O/MeOH (90:10, v/v). Samples were loaded at a flow rate of about one drop per 2 s and, after complete loading, columns were washed with 500 μl H₂O/MeOH (90:10, v/v). The phase was thereafter dried under aspiration, and lipids were eluted with 750 μl MeOH. Solvent was evaporated under N₂, and samples were resuspended with 140 μl

MeOH and transferred into a vial (Macherey-Nagel, Hoerd, France). Finally, the 140 μl of methanol were evaporated and our sample resuspended with 10 μl of methanol for LC-MS analysis. 6-keto-prostaglandin F1 α , thromboxane B₂, prostaglandin E₂, 8-iso prostaglandin A₂, prostaglandin E₃, 15-deoxy- $\Delta^{12,14}$ -prostaglandin J₂ (15d-PGJ₂), prostaglandin D₂ (PGD₂), lipoxin A₄ (LxA₄), lipoxin B₄, resolvin E₁, resolvin D₁, resolvin D₂, resolvin D₃, resolvin D₅ (RvD₅), 7-Maresin 1, leukotriene B₄ (LtB₄), leukotriene B₅ (LtB₅), protectin Dx, 18-HEPE, 5,6-diHETE, 9-HODE, 13-HODE, 15-HETE, 12-HETE, 8-HETE, 5-HETE, 17-hydroxydocosahexaenoic acid (17-HDoHE), 14-HDoHE, 14,15-epoxyeicosatrienoic acid (14,15-EET), 11,12-EET, 8,9-EET, 5,6-EET, 5-oxoeicosatetraenoic acid, prostaglandin F_{2 α} , 11 β -prostaglandin F_{2 α} , 13-Oxo-9Z,11E-octadecadienoic acid (13-oxoODE), 9-oxoODE, 10-HODE, 9,10-dihydroxy-12-octadecenoic acid (9,10-DiHOME), 12,13-DiHOME, 9-hydroxy-10,12,15-octadecatrienoic acid, 13-hydroxy-9,11,15-octadecatrienoic acid, 9,10,13-trihydroxy-11-octadecenoic acid and 9,12,13-trihydroxy-11E-octadecenoic acid, 3-hydroxyoctanoic acid (C8-3OH), 3-hydroxydecanoic acid (C10-3OH), 3-hydroxydodecanoic acid (C12-3OH), 3-hydroxytetradecanoic acid (C14-3OH), 3-hydroxyhexadecanoic acid (C16-3OH), 3-hydroxyoctadecanoic acid (C18-3OH), 2-hydroxyhexadecanoic acid (C16-2OH), 2-hydroxyoctadecanoic acid (C18-2OH), C12-asparagine- γ -aminobutyric acid, C12-asparagine, C14-asparagine- γ -aminobutyric acid, C14-asparagine, and C14-asparagine-valine were quantified in bacteria, mouse colons, bloods, and BAT. To simultaneously separate the 57 lipids of interest and three deuterated ISs (5-HETEd8, LxA4d4, and LtB4d4), LC-MS/MS analysis was performed on an ultrahigh-performance liquid chromatography system (UHPLC; Agilent LC1290 Infinity) coupled to an Agilent 6460 triple quadrupole MS (Agilent Technologies) equipped with electrospray ionization operating in negative mode. Reverse-phase UHPLC was performed using a Zorbax SB-C18 column (Agilent Technologies) with a gradient elution. The mobile phases consisted of water, acetonitrile (ACN), and formic acid (FA) [75:25:0.1 (v/v/v)] (solution A) and ACN and FA [100:0.1 (v/v)] (solution B). The linear gradient was as follows: 0% solution B at 0 min, 85% solution B at 8.5 min, 100% solution B at 9.5 min, 100% solution B at 10.5 min, and 0% solution B at 12 min. The flow rate was 0.4 ml/min. The autosampler was set at 5°C , and the injection volume was 5 μl . Data were acquired in multiple reaction monitoring mode with optimized conditions (supplemental Table S1). Peak detection, integration, and quantitative analysis were performed with MassHunter Quantitative analysis software (Agilent Technologies). Blank samples were evaluated, and their injection showed no interference (no peak detected), during the analysis. For each standard, calibration curves were built using 10 solutions at concentrations ranging from 0.95 to 500 ng/ml.

PUFA “epoxy” metabolites profiling. Metabolites were quantified from bacteria, mouse colons, and BAT by MS after lipid extraction as described above except that 30% of MeOH instead of 10% was used for sample preparation, plate conditioning, and washing. 9,10-epoxyoctadecenoic acid (9,10-EpOME), 12,13-EpOME, 5,6-EET, 8,9-EET, 11,12-EET, 14,15-EET, 5,6-dihydroxy-8,11,14-eicosatrienoic acid, 8,9-dihydroxy-5,11,14-eicosatrienoic acid, 11,12-dihydroxy-5,8,14-eicosatrienoic acid, 14,15-dihydroxy-5,8,11-eicosatrienoic acid, 7,8-epoxydocosapentaenoic acid (7,8-EpDPE), 10,11-EpDPE, 13,14-EpDPE, 16,17-EpDPE, 19,20-EpDPE, 7,8-dihydroxydocosapentaenoic acid (7,8-DiHDPE), 10,11-DiHDPE, 13,14-DiHDPE, 16,17-DiHDPE, 19,20-DiHPE, 8,9-epoxyeicosatetraenoic acid (8,9-EpETE), 11,12-EpETE, 14,15-EpETE, 17,18-EpETE, 8,9-DiHETE, 11,12-dihydroxyeicosatetraenoic acid, 14,15-dihydroxyeic

osatetraenoic acid, and 17,18-dihydroxyeicosatetraenoic acid were quantified in bacteria, mouse colons, and BAT. To simultaneously separate 28 lipids of interest and three deuterated ISs (5-HETEd8, Lx44d4, and LtB4d4), LC-MS/MS analysis was performed on an UHPLC (Agilent LC1290 Infinity) coupled to an Agilent 6460 triple quadrupole MS (Agilent Technologies) equipped with electrospray ionization operating in negative mode. Reversed-phase UHPLC was performed using a Zorbax SB-C18 column (Agilent Technologies) with a gradient elution. The mobile phases consisted of water, ACN, and FA [75:25:0.1 (v/v/v)] (solution A) and ACN and FA [100:0.1 (v/v)] (solution B). The linear gradient was as follows: 30% solution B at 0 min, 73.5% solution B at 13 min, 100% solution B at 13.10 min, 100% solution B at 16 min, 30% solution B at 16.1 min, and 30% of solution B at 18 min. The flow rate was 0.4 ml/min. The autosampler was set at 5°C, and the injection volume was 5 µl. Data were acquired in multiple reaction monitoring mode with optimized conditions (supplemental Table S2). Peak detection, integration, and quantitative analysis were performed with MassHunter Quantitative analysis software (Agilent Technologies). Blank samples were evaluated, and their injection showed no interference (no peak detected), during the analysis.

Gene expression analysis by real-time qPCR analysis and RNAseq analysis

Total RNA was prepared from tissues using TriPure reagent (Roche). Quantification and integrity analysis of total RNA was performed by running 1 µl of each sample on an Agilent 2100 Bioanalyzer (Agilent RNA 6000 Nano Kit, Agilent).

For qPCR analysis, cDNA was prepared by reverse transcription of 1 µg total RNA using a Reverse Transcription System kit (Promega, Leiden, The Netherlands). Real-time PCRs were performed with the StepOnePlus real-time PCR system and software (Applied Biosystems, Den IJssel, The Netherlands) using Mesa Fast qPCR SYBR Green mix (Eurogentec, Seraing, Belgium) for detection according to the manufacturer's instructions. RPL19 was chosen as housekeeping gene. All samples were run in duplicate in a single 96-well reaction plate, and data were analyzed according to the $2^{-\Delta\Delta C_t}$ method. The identity and purity of the amplified product were checked through analysis of the melting curve carried out at the end of amplification. Primer sequences for the targeted mouse genes are available in supplemental Table S3.

MPO activity

The tissue-associated MPO assay was performed to quantify the degree of neutrophil infiltration as previously described (16). Briefly, tissue was placed in hexadecyltrimethylammonium bromide buffer (0.5% hexadecyltrimethylammonium bromide in 50 mM potassium phosphate buffer, pH 6) on ice and homogenized. The homogenate was centrifuged at 18,000 g for 20 min at 4°C. Seven microliters of supernatant, in duplicate, were then added to 96-well plates together with 200 µl of a solution of σ -dianisidine (0.167 mg/ml) and hydrogen peroxide (500 ppm) in potassium phosphate buffer (50 mM, pH 6). Total protein concentration was determined using the detergent compatible protein assay (Bio-Rad, Nazareth, Belgium). MPO activity in the supernatant was measured at 460 nm and normalized for protein concentration. Results are expressed as percentage of vehicle.

Cytokine quantification by ELISA

Levels of interleukin-6 (IL-6) in the colon were determined by a sandwich-type ELISA technique using the Ready-Set-Go!

Kit (eBioscience, Vienna, Austria) following the manufacturer's instructions. Total protein concentration was determined using the detergent compatible protein assay before the ELISA assays were run.

Statistical analyses

Statistical analyses were performed using GraphPad Prism version 9.4.0 (GraphPad Software, San Diego, CA) and RStudio 2022.07.1 for MacOS. Comparison between three or more groups on one time point was performed by one-way ANOVA, followed by Tukey correction and comparison between three or more groups at different time points was performed by two-way repeated measures ANOVA. $P < 0.05$ was considered statistically significant. Outliers were tested and removed using ROUT test, when $P < 0.01$ (Prism 9.4v). We used Rstudio program to perform the bubble plots using the packages tidyverse, dplyr, and ggplot2. To perform the volcano plot, we used the ggrepel package on RStudio. To perform the principal component analysis (PCA) and regularized canonical correlation analysis (rCCA), we used the FactoMineR, factoextra, clusterSim, BBmisc, and MixOmics packages on Rstudio. We used Rstudio program to perform the correlation matrices using tidyverse, dplyr, ggplot2, corr, corrplot, Hmisc, and psych packages. Correlation analyses were assessed by Spearman's correlation tests, followed by a Holm's adjustment for multiple testing.

RESULTS

D. welbionis J115^T prevents diet-induced obesity and ameliorates the glycemic profile

We confirmed that the administration of *D. welbionis* J115^T significantly reduced HFD-induced body weight and fat mass gain (Fig. 1A, B). The lower fat mass gain was associated with an overall reduction (35%–50%) in the weight of the different white adipose tissues (visceral adipose tissue, epididymal adipose tissue, and subcutaneous adipose tissue) (Fig. 1C).

To further explore whether the lower fat mass was associated with changes in glucose metabolism, we performed an oral glucose tolerance test. We found that *D. welbionis* J115^T-treated mice exhibited an improved glucose excursion, with a significant normalization of the glycemia at the end of the 2 h period (Fig. 1D). This effect was associated with significantly lower fasted insulinemia, both at baseline and 15 min after glucose administration (Fig. 1E). Consequently, *D. welbionis* J115^T abolished HFD-induced insulin resistance index (Fig. 1F).

D. welbionis J115^T produces several lipids linked with beneficial effects

To further decipher the potential mechanisms by which *D. welbionis* J115^T acts on host metabolism, we first investigated total fatty acids by MS after liquid extraction; 21 were quantifiable in the whole bacterium. As a benchmark, we used the probiotic bacterium EcN, which is known to have anti-inflammatory properties (11). Among the lipids, six were very low or not detected in the membrane of *D. welbionis* J115^T as compared to

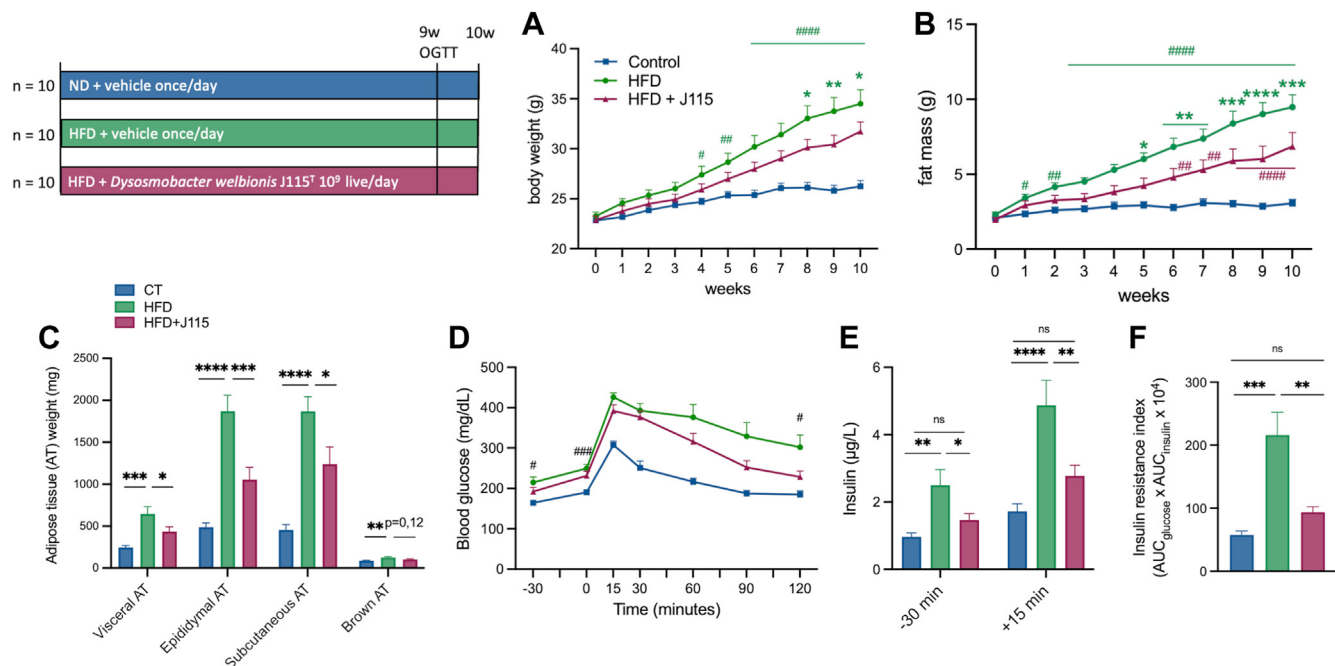


Fig. 1. *Dysosmobacter welbionis* J115^T alleviates diet-induced obesity along with an improvement of the glucose intolerance. (A and B) Body weight and fat mass evolution during 10 weeks of mice fed a normal (ND) or high-fat diet (HFD) either treated with a daily oral gavage of vehicle or live *D. welbionis* J115^T 1x10⁹ colony-forming units (cfus) frozen in trehalose. (C) Weight at the end of the 10 weeks of the white adipose tissues: visceral AT, epididymal AT, subcutaneous AT, and brown AT. (D) Plasma glucose profile during a two-hour oral glucose tolerance test (OGTT). (E) Plasma insulin levels 30 min before and 15 min after glucose administration. (F) Insulin resistance index. Number of mice per group: 9–10. Data were analyzed using one-way ANOVA followed by Tukey's post hoc test for figure parts C–E and two-way ANOVA followed by Tukey's post hoc test for figure parts A, B, and D. **P* < 0.05; ***P* < 0.01; and ****P* < 0.001. Results are represented as bar plots with mean ± SEM for figure parts C, E, and F. In figure A and B, * are for comparisons between the high-fat diet (HFD) versus HFD + J115 group and # are for comparisons for the HFD and the control (CT) or for the HFD+J115 and the CT.

EcN, whereas other lipids were almost only detected in *D. welbionis* J115^T (Fig. 2A, B). Interestingly, C18:2 n-6, precursor of the DiHOME family of lipids, was detected in higher amount than EcN, where it was not detected (Fig. 2A, B).

Next, amongst the 85 lipids quantified by our two methods (supplemental Tables S1 and S2), the concentration of 21 (i.e., PUFA metabolites, hydroxylated on the second or the third carbon, or specific lipopeptides) of them was above the limit of quantification. As shown on the Fig. 2C, among the 21 bioactive lipids analyzed in vitro, 19 were highly concentrated in the pellet of *D. welbionis* J115^T compared to EcN (2–60 times higher), except for C14-3OH and C14-asparagine. Among the most affected, *D. welbionis* J115^T produced a very high amount of 12,13-DiHOME in the *D. welbionis* J115^T samples with a mean of 33,781 pg/mg of protein in the cell pellet (Fig. 2D). The quantity was also increased in the supernatant after fermentation, ranging from 1619 ± 154 to 741,157 ± 60,361 pg/ml (Fig. 2D). Strikingly, 12,13-DiHOME has recently been identified as an oxylipin and is currently investigated in metabolic diseases for its effects as stimulator of BAT activity (17–19). Among the other lipids, the C18-3OH is also increased in *D. welbionis* J115^T compared to EcN. This lipid is particularly interesting as it has PPAR-γ-activating properties

(11). We also measured the differential abundance in the culture medium of *D. welbionis* J115^T prior and after fermentation. As shown in Fig. 2D, we observed that although the abundance C18-3OH was high in the bacterium and the supernatant, it might result of accumulation due to its higher concentration in the sterile culture medium. However, for the 12,13-DiHOME, this lipid was lower to nonexistent in the sterile medium than the fermented medium, suggesting the implication of *D. welbionis* J115^T in its production. The 9,10-DiHOME, 9,10,13-trihydroxy-11-octadecenoic acid, and 9,12,13-trihydroxy-11E-octadecenoic acid had the same quantitative profile as the 12,13-DiHOME (Fig. 2D).

D. welbionis J115^T abolishes HFD-induced whitening of the BAT and changes bioactive lipids profile

Given that, in vitro, *D. welbionis* J115^T produces high levels of 12,13-DiHOME and other bioactive lipids associated with BAT activity and energy metabolism, we further investigated in vivo its effects on the BAT of the treated mice. Although the decrease in the BAT weight was not significant, we found that *D. welbionis* J115^T significantly reduced the whitening of BAT induced by the HFD (Fig. 2E, F). Indeed, as shown by the histological analysis, *D. welbionis* J115^T decreased lipid

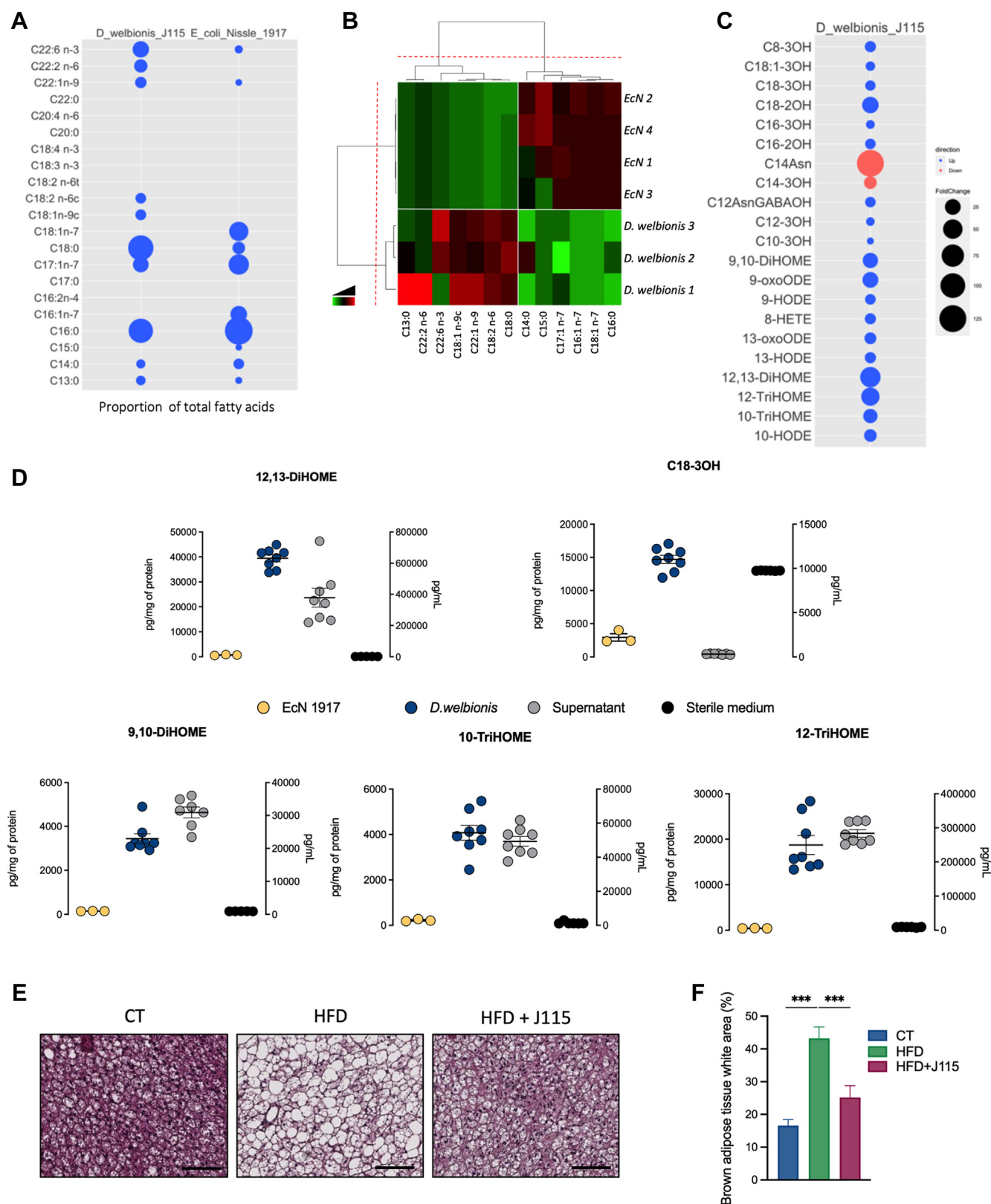


Fig. 2. *Dysosmobacter welbionis* J115^T produces several bioactive lipids and modifies the brown adipose tissue morphology. (A and B) Parts A and B show a bubble plot (A) and heatmap (B) showing the relative abundance of several fatty acids comparing *D. welbionis* J115^T and *Escherichia coli* Nissle 1917 (EcN). Values were measured in % of total fatty acids. (C) Bubble plot representing the fold change increase or decrease of abundance in pg/mg of protein in *D. welbionis* J115^T comparing to EcN. (D) Abundance of 12,13-DiHOME, C18-3OH, 9,10-DiHOME, 10-TriHOME, and 12-TriHOME in the culture medium (sterile or fermented) of *D. welbionis* J115^T in pg/mL and at the bacterial level (of *D. welbionis* J115^T or *Escherichia coli* Nissle 1917) in pg/g of protein. (E) Representative H&E-stained pictures of BAT. Scale bar = 100 μ m. (F) Percentage of white area on the slices, corresponding to lipid droplets, in the BAT. Number of measures

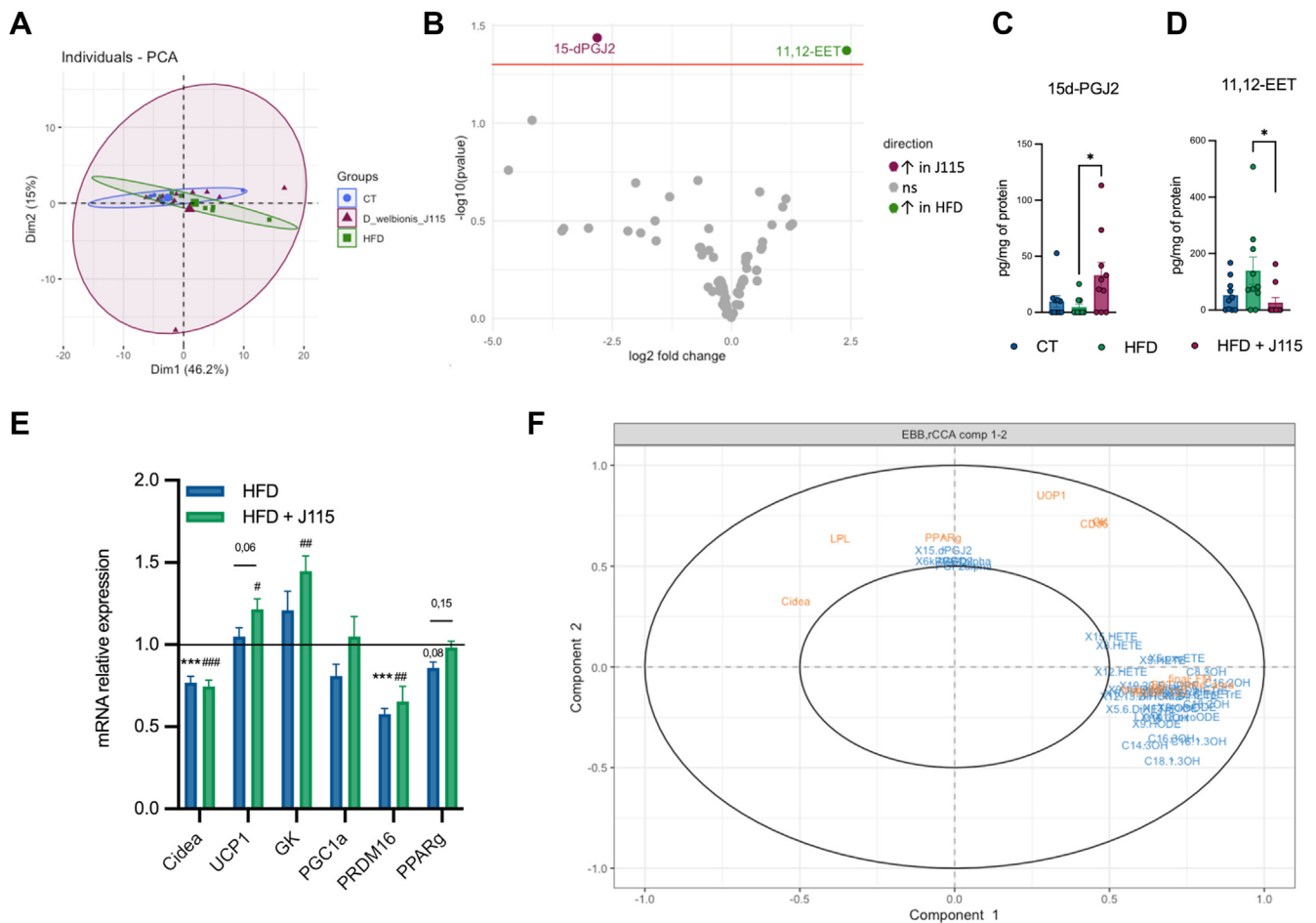


Fig. 3. *Dysosmobaracter welbionis* J115^T-induced lipid changes in the brown adipose tissue. (A) Principal component analysis showing the distribution of individuals based on their brown adipose tissue lipid profile. (B) Volcano plot with the bioactive lipid fold change in the brown adipose tissue. (C) Changes in 15d-PGJ₂. (D) Changes in 11,12-EET. (E) mRNA expression of PPARγ related genes relative to the control group. (F) Regularized canonical correlation analysis including metabolic parameters, mRNA relative expression, and lipids in the brown adipose tissue. Number of mice per group: 9–10. Data were analyzed using one-way ANOVA followed by Tukey's post hoc test for figure parts C–E. **P* < 0.05; ***P* < 0.01; and ****P* < 0.001. Results are represented as mean ± SEM for figure parts C–E. 15d-PGJ₂, 15-deoxy-Δ^{12,14}-prostaglandin J₂; EET, epoxyeicosatrienoic acid; PPAR, peroxisome proliferator-activated receptor.

droplet size and white-like appearance of the BAT. The quantification of the white area was 45% lower in *D. welbionis* J115^T-treated mice than the HFD. It is worth noting that this effect of *D. welbionis* J115^T has been linked to a higher mitochondrial number and activity (13). We then explored whether daily administration of *D. welbionis* J115^T for several weeks could also affect the lipidomic profile of the BAT. We measured 83 bioactive lipids in the BAT and using PCA and volcano plot, we found that the overall lipidome was not shifted between the HFD group and J115^T-treated group (Fig. 3A, B), excepting for two lipids that were markedly affected. The lipid 15d-PGJ₂ was increased by 700% in *D. welbionis* J115^T-treated mice as compared to HFD-fed mice (Fig. 3C), whereas 11,12-EET was decreased by

500% in the BAT of *D. welbionis* J115^T as compared to HFD-fed mice (Fig. 3D).

15d-PGJ₂ is a metabolite of arachidonic acid (AA), a 20:4 n-6 fatty acid. Interestingly, 15d-PGJ₂ has been shown to have a strong affinity for PPAR-γ (20, 21). This nuclear receptor is involved in several biological functions, such as the control of the expression of several genes involved in BAT metabolism such as the uncoupling protein-1 (*Ucp1*), the PPAR-γ coactivator 1α, the proline-rich domain containing 16 (*Prdm16*), which are all involved in mitochondria biogenesis, thermogenesis processes, and eventually energy expenditure in AT (22). Accordingly, we found that several genes controlled by PPAR-γ tended to or were significantly upregulated in *D. welbionis* J115^T-treated mice as

per lipid: six in the sterile medium, eight in the fermented medium, eight in *D. welbionis* J115^T, and three in *Escherichia coli* Nissle 1917. Number of mice per group: 9–10. Data were analyzed using one-way ANOVA followed by Tukey's post hoc test for figure parts D and F. **P* < 0.05; ***P* < 0.01; and ****P* < 0.001. Results are represented as mean ± SEM for figure parts D and F. 10-TriHOME, 9,10,13-trihydroxy-11-octadecenoic acid; 12-TriHOME, 9,12,13-trihydroxy-11E-octadecenoic acid; DiHOME, dihydroxy-12-octadecenoic acid.

compared to HFD-fed mice (Fig. 3E). This is consistent with the observed effect on the BAT morphology but also with the conclusion from the rCCA, highlighting correlations between two datasets acquired on the same experiment. Similarly as PCA, rCCA seeks for linear combination between variables, while trying to maximize these correlations (Fig. 3F). Interestingly, this analysis strongly confirmed that 15d-PGJ₂ correlated with PPAR- γ and genes related to the BAT activity (Fig. 3F), whereas most of the other lipids were positively correlated with the final BW, final fat mass, insulin resistance index, and whitening of the BAT (Fig. 3F). On the other hand, the 11,12-EET was decreased by *D. welbionis* J115^T treatment.

D. welbionis J115^T increases the abundance of 15d-PGJ₂, RvD5, and 10,11-EpDPE in the colon

Because *D. welbionis* J115^T produces different bioactive lipids, we sought to investigate whether the treatment induced a shift in the colonic lipid profile, where the bacterium is directly in contact with the tissue. For this, we performed a similar analysis as the one done in the BAT. We analyzed 83 bioactive lipids and performed a PCA between the HFD group and the *D. welbionis*

J115^T-treated group (Fig. 4A). As for the BAT, we did not observe any shift in the colon lipid profile following *D. welbionis* J115^T supplementation (Fig. 4A). However, when using the volcano plot (Fig. 4B), we identified three specific lipids that were significantly increased upon *D. welbionis* J115^T treatment compared to HFD mice. First, we found a higher abundance of 10,11-EpDPE in *D. welbionis* J115^T-treated mice (Fig. 4B, C). Next, we also found that the level of the RvD5 was decreased by 60% in the HFD-fed mice but markedly increased by 660%, following *D. welbionis* J115^T supplementation compared to HFD-fed mice (Fig. 4B, D). RvD5 is a lipoxygenase metabolite of DHA (23). This lipid is an attractive inflammation-resolving chemical mediator with its ability to activate host defense system in mice during intestinal inflammation (24, 25). We found that HFD-fed mice exhibited a lower expression of mucin 2 (*Muc2*), the antimicrobial peptide angiotensin 1 (*Ang1*), as well as three histone deacetylases (*Hdac1*, *Hdac2*, and *Hdac3*), nitric oxide synthase 2 (*Nos2*), and PPAR- γ (*Pparg*). Finally, we observed a marked increase of 15d-PGJ₂ in *D. welbionis* J115^T-treated mice (Fig. 4B, E). 15d-PGJ₂ has also been shown to reduce intestinal inflammation in a murine dextran sulfate sodium

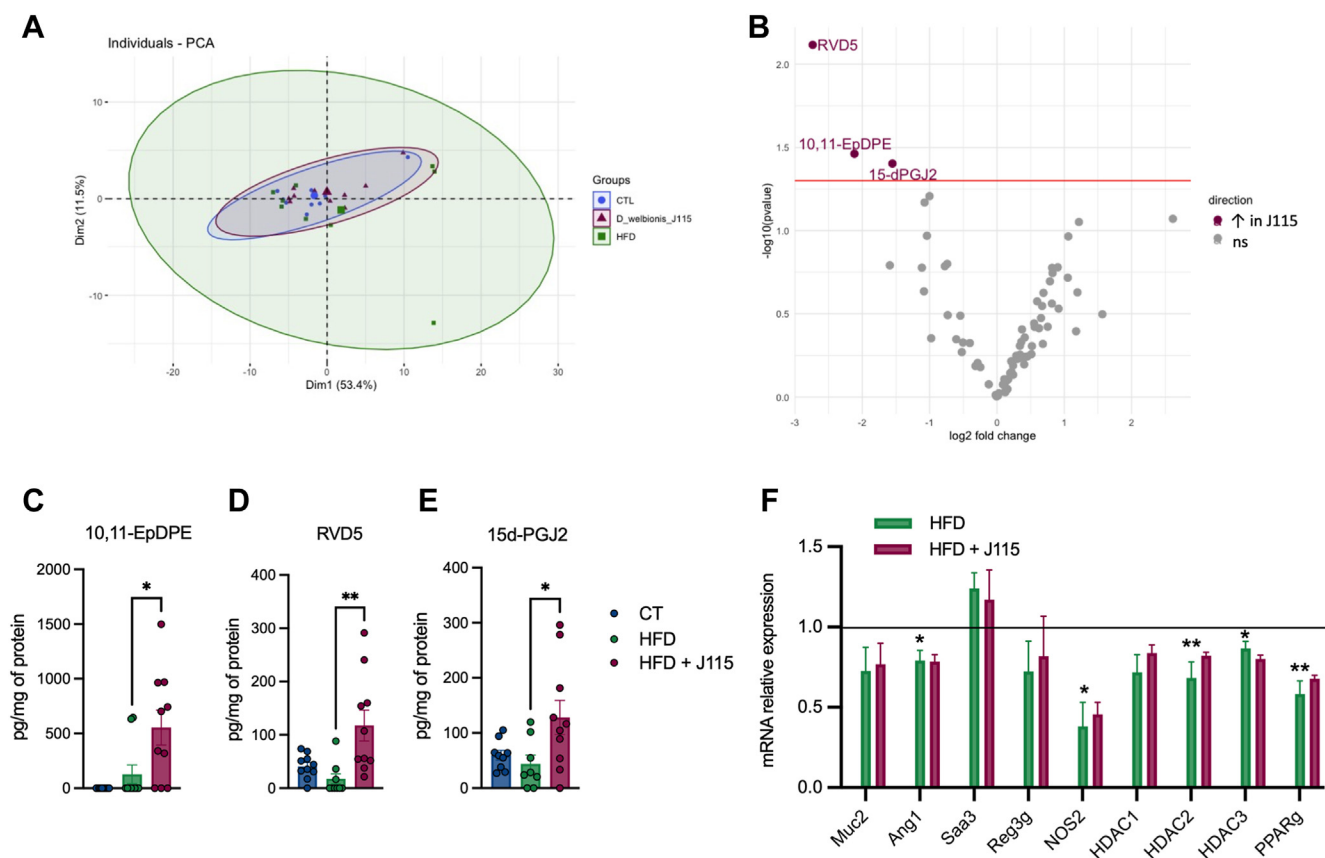


Figure 4. *Dysosmobacter welbionis* J115^T-induced lipid changes in the colon. (A) Principal component analysis showing the distribution of individuals based on their colon lipid profile. (B) Volcano plot with the bioactive lipid fold change in the colon. (C) Changes in 10,11-EpDPE. (D) Changes in RvD5. (E) Changes in 15d-PGJ₂. (F) mRNA relative expression of genes involved in mucus production, inflammation, and gene regulation. Number of mice per group: 8–10. Data were analyzed using one-way ANOVA followed by Tukey's post hoc test for figure parts C–F. **P* < 0.05; ***P* < 0.01; and ****P* < 0.001. Results are represented as mean ± SEM for figure parts C–E. 15d-PGJ₂, 15-deoxy- Δ 12,14-prostaglandin J₂; EpDPE, epoxydocosapentaenoic acid; RvD5, resolvin D5.

(DSS)-induced colitis model (26, 27). It is worth noting that in this study, mice are not developing specific inflammatory phenotype in the colon, as the expression level of the inflammatory marker the serum amyloid A3 (*Saa3*) remains unchanged (Fig. 4F). Given that *D. welbionis* J115^T markedly increased the colonic content of two interesting bioactive lipids with anti-inflammatory properties in our study, we tested whether the administration of *D. welbionis* J115^T could reduce DSS-induced inflammation. In a preliminary experiment, we found that *D. welbionis* J115^T did not affect DSS-induced body weight loss after one week of *D. welbionis* J115^T pretreatment (supplemental Fig S1A). Conversely, *D. welbionis* J115^T significantly reduced the weight over length (W/L) ratio, a key marker of colitis. MPO activity, a marker of neutrophil recruitment, was also decreased, as was decreased the colonic content of (IL-6) (supplemental Fig S1B–D), thereby confirming potential anti-inflammatory properties.

***D. welbionis* J115^T supplementation changes several blood lipids with potential metabolic effects**

To complement the analyses performed in colon and BAT, we performed a similar analysis in the plasma. When performing a PCA, we observed that the overall lipidome was not shifted between the three different groups. But by analyzing each lipid distribution separately (Fig. 5A), we first measured a normalization in the levels of the prostaglandin D2 (PGD₂) following *D. welbionis* J115^T treatment, which is the precursor of 15d-PGJ₂ (Fig. 5B). However, we observed a significant decrease in the levels of 15d-PGJ₂ in the HFD group and this was even more pronounced in the *D. welbionis* J115^T treated group (Fig. 5C). We measured a 3-fold increase of 17-HDoHE, a precursor of RvD5 and PPAR γ agonist (28), in *D. welbionis* J115^T-treated group compared to HFD (Fig. 5D). Hydroxylated lipids 2-hydroxyoctadecanoate (C18-2OH), 3-hydroxyhexadecanoate (C16-3OH) and 3-hydroxymyristate (C14-3OH) were all significantly decreased by *D. welbionis* J115^T supplementation in the plasma (Fig. 5E–G). The 3-hydroxyoctadecanoate (C18-3OH) was significantly decreased following HFD treatment and increased with *D. welbionis* J115^T supplementation (Fig. 5H). *D. welbionis* J115^T supplementation increased C18-3OH levels in the plasma (Fig. 5H). This lipid was highly present at the level of the bacteria and in the supernatant, and is a potent PPAR- γ -activator with anti-inflammatory effects demonstrated in the colon (11).

Apart from these, we found an increase in several other bioactive lipids. The 14,15-EET was significantly increased by *D. welbionis* J115^T treatment (Fig. 5I), and 14,15-EET generated from AA by cytochrome P450 epoxygenases is a PPAR agonist and has beneficial effects on insulin resistance, cardiovascular diseases and inflammation (29–32). The lipid 12-HETE, which is a PPAR- γ agonist (33), was significantly decreased following HFD treatment and increased with *D. welbionis* J115^T supplementation (Fig. 5J), this lipid has been

shown to reduce fasted glycemia, AT inflammation and to improve glucose tolerance in obese and diabetic mice (33). Both 9- and 13-oxo-octadecadienoic acid (9- and 13-oxo-ODE) were decreased in *D. welbionis* J115^T-treated group compared to control and HFD group (Fig. 5K, L), both derived from linoleic acid. Finally, 9 and 10-hydroxy-octadecadienoic acid (9-HODE and 10-HODE) were significantly decreased by *D. welbionis* J115^T compared to control and HFD group (Fig. 5M, N), these lipids have been shown to be higher in several diseases such as obesity, diabetes, cardiovascular diseases and inflammation (34–36). Altogether, these data contribute to the understanding of the beneficial effects of *D. welbionis* J115^T and uncover potential beneficial bioactive lipids circulating in the blood of treated mice, despite not depicting a complete picture.

DISCUSSION

In this study, we first confirmed that *D. welbionis* J115^T reduces HFD-induced body weight gain, fat mass gain, and glucose intolerance. We further discovered that *D. welbionis* J115^T produces numerous lipids among which bioactive lipids known to act on energy metabolism by increasing BAT activity and to have anti-inflammatory properties. Interestingly, EcN has been used as a probiotic and shown to produce several bioactive lipids (11, 37). By comparing the composition of the free fatty acids of *D. welbionis* J115^T with EcN, we discovered that *D. welbionis* J115^T not only produces similar families of fatty acids and in a much larger proportion, but between 2 and 60 times higher levels than EcN.

Among them, we found that *D. welbionis* J115^T produces a very large quantity of 12,13-DiHOME compared to the other lipids measured (40,000 compared to 0–20 000 pg/mg of protein for the other lipids). This lipokine is known to induce thermogenic activities, following a cold exposure or physical exercise (17, 18). Whether the effects of *D. welbionis* J115^T are due to the production of this specific bioactive lipid remains to be proven. However, we found that besides the lower fat mass, *D. welbionis* J115^T-treated mice also displayed a lower whitening of the BAT. We also previously discovered that *D. welbionis* J115^T increased the number of mitochondria in the BAT of HFD-treated mice (13), thereby suggesting a putative link with the production of 12,13-DiHOME. Whether *D. welbionis* J115^T is one of the key bacteria producing 12,13-DiHOME in the gut remains unknown. For the production of 12,13-DiHOME from 12,13-EpOME, the bacterial enzyme serum epoxide hydrolase has not been identified in *D. welbionis* J115^T genome, suggesting that another mechanism is implicated in its synthesis.

We also observed an overall increase of lipids hydroxylated on the second and third carbon. In the genome of *D. welbionis* J115^T, we found several enzymes involved in the synthesis pathway of these lipids such as

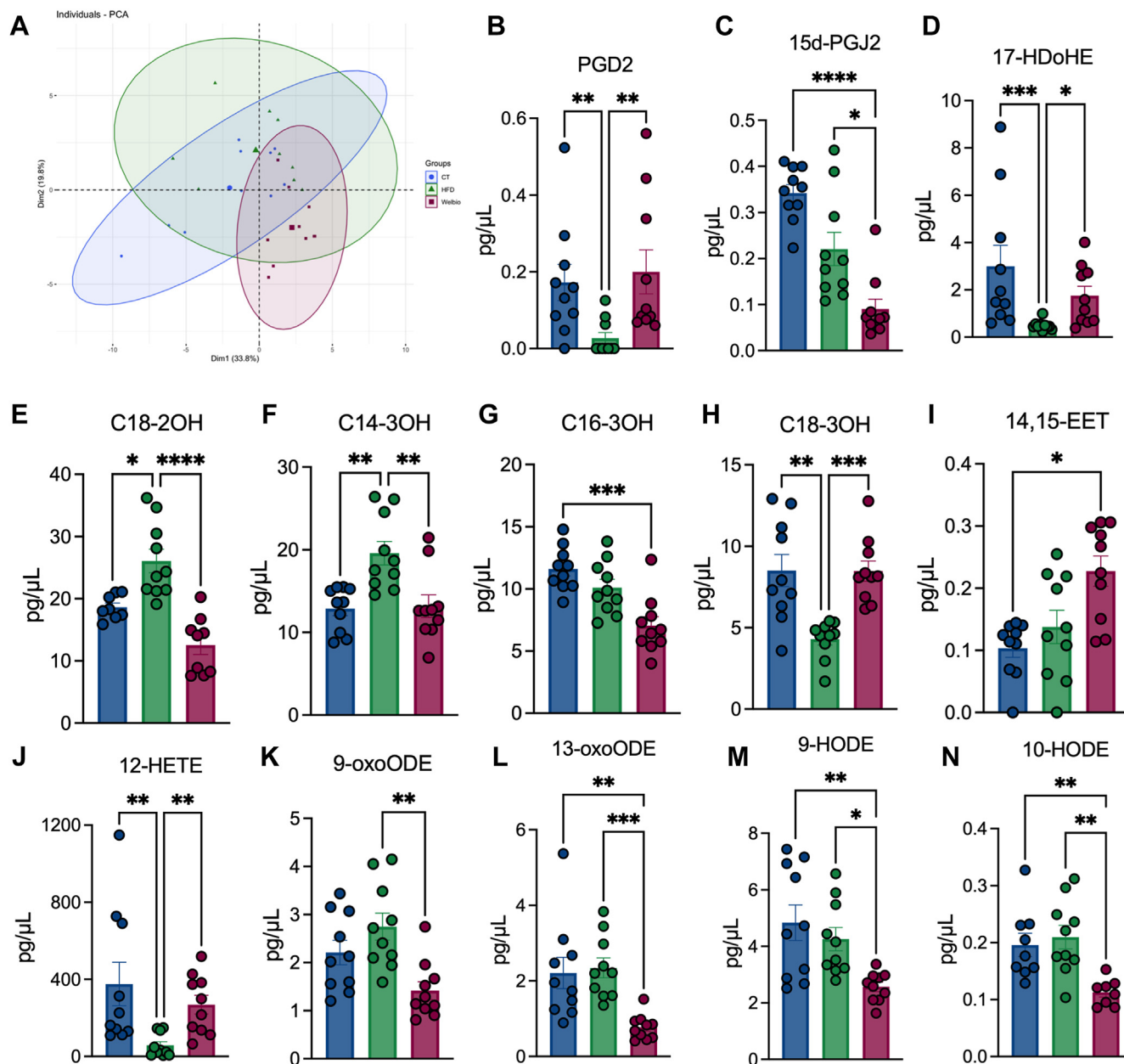


Fig. 5. *Dysosmibacter welbionis* J115^T-induced lipid changes in the blood. (A) Principal component analysis showing the distribution of individuals based on their plasma lipid profile. (B) Changes in PGD2. (C) Changes in 15d-PGJ2. (D) Changes in 17-HDoHE. (E) Changes in C18-2OH. (F) Changes in C14-3OH. (G) Changes in C16-3OH. (H) Changes in C18-3OH. (I) Changes in 14,15-EET. (J) Changes in 12-HETE. (K) Changes in 9-oxoODE. (L) changes in 13-oxoODE. (M) Changes in 9-HODE. (N) Changes in 10-HODE. Statistical comparisons were either HFD versus CT or HFD+J115 versus CT. Number of mice per group: 8–10. Data were analyzed using one-way ANOVA followed by Tukey's post hoc test **P* < 0.05; ***P* < 0.01; ****P* < 0.001, and *****P* < 0.0001. Results are represented as mean ± SEM. 15d-PGJ₂, 15-deoxy-Δ^{12,14}-prostaglandin J₂; EET, epoxyeicosatrienoic acid; HDoHE, hydroxydocosaheptaenoic acid; HFD, high-fat diet; oxoODE, hydroxyoctadecadienoic acid; PGD₂, prostaglandin D₂.

alpha/beta hydrolases (data not shown). Among these lipids, we noticed that *D. welbionis* J115^T contains a large amount of the long-chain fatty C18-3OH, a lipid that we already identified as anti-inflammatory and produced by EcN (11). We previously showed that the oral administration of C18-3OH decreased a DSS-induced colitis in mouse and discovered that C18-3OH is a PPAR-γ agonist (11). Strikingly, this lipid is five times more produced by *D. welbionis* J115^T than EcN. The high level of C18-3OH in the culture medium suggests the

potential of *D. welbionis* J115^T to accumulate this lipid during the culturing process, and thereby potentially contributing to its beneficial effects observed in vivo. Whether *D. welbionis* J115^T is able to produce this lipid remains unclear. In the genome of *D. welbionis* J115^T, alpha/beta hydrolase enzymes have been identified and can be implicated in the formation of C18-3OH. On the other hand, this fatty acid has been shown to be part of the lipid A in lipopolysaccharides and therefore it is plausible that *D. welbionis* J115^T as Gram-negative

bacterium accumulates and or produces C18-3OH. But still, it remains to investigate the exact lipopolysaccharides composition of *D. welbionis* J115^T.

To further decipher whether *D. welbionis* J115^T treatment modified the lipid profile in different organs, we next measured 78 lipids in the BAT, the colon and in the blood. Interestingly, we observed an increase in C18-3OH in the plasma of mice receiving *D. welbionis* J115^T treatment. Suggesting that the bacterium is not only able to increase C18-3OH in vitro but also in vivo. In the plasma, we also found an increase in 9-oxoODE and 13-oxoODE. These lipids are positively associated with metabolic syndrome (38), and 13-oxo-ODE has PPAR γ -activating properties (39). Similarly, the lipids 9- and 10-HODE are also increased in pathological conditions such as diabetes, obesity and cancer, and 9-HODE has been shown to decrease following healthy diets and loss of body weight (35, 36). 10-HODE is positively associated with fasting glucose plasma levels and plasma glucose levels after glucose administration during an oral glucose tolerance test, which makes this lipid suitable as biomarker for the early detection of impaired glucose tolerance (40). Two other derivatives of AA were increased by that *D. welbionis* J115^T supplementation, namely 12-HETE and 14,15-EET. Both lipids are implicated in obesity, diabetes and 14,15-EET also shows potential anti-inflammatory properties, potentially mediated by its PPAR agonist properties (29). Interestingly, 12-HETE has been recently identified as a new enterosyne (i.e., active molecule acting in the gut environment) and is known as the second messenger of the enkephalin/MOR pathway acting on PPAR γ in different organs (e.g., brain, liver, AT) thereby reducing glycemia, inflammation and improving glucose metabolism (33).

Three hydroxylated lipids, namely C18-2OH, C14-3OH and C16-3OH, were decreased in the blood following *D. welbionis* J115^T treatment. However, this observation may simply be a reflect of the increased adiposity in HFD treatment and is therefore decreased upon *D. welbionis* J115^T supplementation along with decreased measured adiposity in our mice. Nevertheless, C14-3OH is a lipid enriched in obese patients with T2D mellitus and is associated with fasting glucose, glycated hemoglobin and HOMA-IR (41, 42). Interestingly, C18-2OH was shown to be increased in high-risk cardiovascular disease diabetic patients (43) and patients with BMI exceeding 25 (44), just as C14-3OH is a lipid enriched in obese patients with T2D mellitus (41, 42).

In the BAT, we found that two lipids were significantly changed by *D. welbionis* J115^T. The lipid 11,12-EET was increased by the HFD and decreased upon *D. welbionis* J115^T supplementation. This AA derivate has been proposed to improve wound healing in *ob/ob* mice (45). We also found a marked increase of 15d-PGJ₂, a member of the cyclopentenone prostaglandin (PG) group. PG are key mediators of inflammation and their production changes during the different stages of

inflammation. Cyclopentenone PG are produced to terminate inflammation with their immunomodulatory and anti-inflammatory properties (46). 15d-PGJ₂ is a strong PPAR γ agonist, therefore we measured several targets of this nuclear receptor increased in mice treated with *D. welbionis* J115^T. Accordingly, in the present study, we found a higher expression of several genes involved in BAT activity. Overall, several lipids either produced by *D. welbionis* J115^T or increased in the tissues of treated mice are PPAR γ agonists, suggesting that the observed beneficial effects on the metabolism are at least partially due to a modulation of this target's activity. Given that the two lipids derive from AA that has not been found at the level of the bacteria, we cannot state if the changes in lipids measured in the BAT are due to production of these lipids by the bacteria after oral administration, or if they are an indirect effect of BAT responding to the administration of *D. welbionis* J115^T.

The same 83 lipids were analyzed as well in the colon and three of them were significantly changed upon *D. welbionis* J115^T treatment. The 10,11-EpDPE is strongly increased by *D. welbionis* J115^T. This bioactive lipid has been shown to have antihyperalgesic effects (47) and to be negatively associated with major depression scores in type 2 diabetic patients. People with T2D mellitus are at increased risk for depression (48). The second lipid markedly affected was the RvD5, a lipid known as proresolving mediator in intestinal inflammation (25, 49). In our study RvD5 was decreased by the HFD and strongly increased by *D. welbionis* J115^T treatment. RvD5 was not detected in the sterile neither in the sterile culture medium nor in the fermented medium and the bacteria. Therefore, the bacteria cannot take them up and transfer them from the sterile medium, but we may speculate that the bacteria simply stimulate host responses that cause them to be made. Moreover, we found that its precursor 17-HDoHE was increased in the plasma of treated mice. To further elucidate, the mechanism by which *D. welbionis* J115^T increases the precursor and RvD5 might be studied by using different models such as for instance ex vivo approaches using culture of colonic tissue in presence of *D. welbionis* J115^T or intestinal cell lines. However, given that the precursor of RvD5 was increased in the plasma of *D. welbionis* J115^T, we may not exclude that the source may come from other tissues or even from multiple organs. Although, we found a higher abundance of 10,11-EpDPE in the colon of *D. welbionis* J115^T-treated mice, this lipid was not detected in the sterile medium and in the bacteria, thereby suggesting that the origin was not directly *D. welbionis* J115^T but rather a change from the host production. 10,11-EpDPE is produced from DHA C22:6n-3 fatty acids that are highly produced in *D. welbionis* J115^T compared to EcN (Fig. 2B).

Furthermore, in the colon we observed an increase in 15d-PGJ₂, a lipid also higher in the BAT of *D. welbionis* J115^T-treated mice and known to have anti-


inflammatory properties. For instance, this lipid has been shown to ameliorate DSS-induced colitis in mice (26, 27). Similarly to BAT, the increase of these lipids may derive from the culture of *D. welbionis* J115^T, but also could be due to changes in the colon following *D. welbionis* J115^T administration. In this scope, we measured in the blood an increase in the 15d-PGJ₂ precursor PGD₂ following *D. welbionis* J115^T treatment, but a decrease of 15d-PGJ₂. However, research shows that the levels of 15d-PGJ₂ in plasma of diabetic patients was increased compared to control plasma (50), potentially showing different effect in the plasma compared to tissues. In a previous study, we observed a reduction of this specific lipid in DSS-induced colitis in mice (51). However, in the present study, the HFD treatment was not sufficient to induce an inflammatory phenotype in the colon, hence potentially not enabling *D. welbionis* J115^T to exert specific anti-inflammatory effects.

However, since two lipids augmented in the *D. welbionis* J115^T supplemented mice colon have anti-inflammatory properties and that *D. welbionis* J115^T also contains anti-inflammatory mediators such as C18-3OH in vitro, we further investigated whether *D. welbionis* J115^T could induce effects on acute inflammatory mouse model. In a first preliminary experiment, we found that *D. welbionis* J115^T as potential beneficial effects on three key hallmarks of colitis such as W/L ratio, MPO activity, and IL-6 levels in the colonic tissue. Whether these effects are due to one or several lipids produced by *D. welbionis* J115^T warrants further investigation.

Altogether, our data show that the newly isolated commensal bacterium *D. welbionis* J115^T produces numerous bioactive lipids in vitro and increases the production of different lipids known to act on both the BAT and the colon. Whether the effects of these lipids are mediating all the beneficial effects of the bacterium remains unknown. A major limitation of our study is that at this stage we are unable to fully explain the mechanisms related to the endogenous modulation of different bioactive lipids in the colon and the BAT. It remains very challenging to understand exactly how *D. welbionis* J115^T might account for the reported metabolic effects and if these are only related to the modulation of bioactive lipids.

Nevertheless, our findings support that the beneficial effects of *D. welbionis* J115^T are at least associated with the modulation of the abundance of several key bioactive lipids acting on either glucose, lipid, energy metabolism, and inflammation.

Data availability

All data are contained within this article. The raw data will be shared upon request: Contact Patrice D. Cani (UCLouvain, Email: Patrice.cani@uclouvain.be). 

Supplemental data

This article contains [supplemental data](#).

Acknowledgments

We thank A. Puel, S. Genten, H. Danthinne, B. Es Saadi, L. Gesche, and R. M. Goebbels (at UCLouvain, Université catholique de Louvain) for their excellent technical support and assistance.

Author contributions

P. D. C. conceptualization; E. M. d. H., C. P., M. A., C. D., P. L. F., M. V. H., G. G. M., N. C., and P. D. C. data generation; E. M. d. H., M. A., and G. G. M. mouse husbandry and experiments; C. P., P. L. F., and N. C. mass spectrometry; E. M. d. H. and C. D. biostatistics; P. D. C., N. M. D., G. G. M., and N. C. resources; P. D. C. project supervision; P. D. C. and E. M. d. H. writing-original draft; E. M. d. H., C. P., M. A., C. D., P. L. F., N. M. D., M. V. H., G. G. M., N. C., and P. D. C. writing-review and editing.

Author ORCIDs

Emilie Moens de Hase  <https://orcid.org/0000-0001-9621-625X>

Mireille Alhouayek  <https://orcid.org/0000-0002-9193-0718>

Nathalie M. Delzenne  <https://orcid.org/0000-0003-2115-6082>

Matthias Van Hul  <https://orcid.org/0000-0002-5503-107X>

Giulio G. Muccioli  <https://orcid.org/0000-0002-1600-9259>

Nicolas Cenac  <https://orcid.org/0000-0002-1552-7812>

Patrice D. Cani  <https://orcid.org/0000-0003-2040-2448>

Funding and additional information

P. D. C. is recipient of Grants from FNRS (Projet de Recherche PDR-convention: FNRS T.0030.21, CDR-convention: J.0027.22, FRFS-WELBIO: WELBIO-CR-2022A-02, EOS: program no. 40007505) and ARC (action de recherche concertée: ARC19/24-096) and La Caixa (NeuroGut).

Conflict of interest

M. A. is research associate and P. D. C. is honorary research director at FRS-FNRS (Fonds de la Recherche Scientifique). P. D. C. and E. M. d. H. are inventors on patent applications dealing with the use of specific bacteria and components in the treatment of different diseases. P. D. C. was cofounder of The Akkermansia Company SA and Enterosys. The other authors declare that they have no conflicts of interest with the contents of this article.

Abbreviations

15d-PGJ₂, 15-deoxy-Δ^{12,14}-prostaglandin J₂; AA, arachidonic acid; ACN, acetonitrile; AT, adipose tissue; BAT, brown adipose tissue; DiHDPE, dihydroxydocosapentaenoic acid; DiHOME, dihydroxy-12-octadecenoic acid; DSS, dextran sulfate sodium; EcN, Escherichia coli Nissle 1917; EET, epoxyeicosatrienoic acid; EpDPE, epoxydocosapentaenoic acid; EpETE, epoxyeicosatetraenoic acid; EpOME, epoxyoctadecenoic acid; FA, formic acid; HDoHE, hydroxydocosahexaenoic acid; IL, interleukin; IS, internal standard; HFD, high-fat diet; LtB4, leukotriene B₄; MeOH, methanol; MPO, myeloperoxidase; PCA, principal component analysis; PGD₂, prostaglandin D₂; PPAR, peroxisome proliferator-activated receptor; rCCA, regularized canonical correlation analysis; RvD5, resolvin D₅; UHPLC, ultra-high-performance liquid chromatography.

REFERENCES

- de Vos, W. M., Tilg, H., Van Hul, M., and Cani, P. D. (2022) Gut microbiome and health: mechanistic insights. *Gut*, **71**, 1020–1032
- Cani, P. D. (2017) Gut microbiota - at the intersection of everything? *Nat. Rev. Gastroenterol. Hepatol.* **14**, 321–322
- Van Hul, M., Le Roy, T., Prifti, E., Dao, M. C., Paquot, A., Zucker, J. D., et al. (2020) From correlation to causality: the case of Subdoligranulum. *Gut Microbes*, **12**, 1–13
- Cani, P. D., Depommier, C., Derrien, M., Everard, A., and de Vos, W. M. (2022) Akkermansia muciniphila: paradigm for next-generation beneficial microorganisms. *Nat. Rev. Gastroenterol. Hepatol.* **19**, 625–637
- Ottman, N., Davids, M., Suarez-Diez, M., Boeren, S., Schaap, P. J., Martins Dos Santos, V. A. P., et al. (2017) Genome-scale model and omics analysis of metabolic capacities of Akkermansia muciniphila reveal a preferential mucin-degrading lifestyle. *Appl. Environ. Microbiol.* **83**, e01014-17
- Yoon, H. S., Cho, C. H., Yun, M. S., Jang, S. J., You, H. J., Kim, J. H., et al. (2021) Akkermansia muciniphila secretes a glucagon-like peptide-1-inducing protein that improves glucose homeostasis and ameliorates metabolic disease in mice. *Nat. Microbiol.* **6**, 563–573
- Plovier, H., Everard, A., Druart, C., Depommier, C., Van Hul, M., Geurts, L., et al. (2017) A purified membrane protein from Akkermansia muciniphila or the pasteurized bacterium improves metabolism in obese and diabetic mice. *Nat. Med.* **23**, 107–113
- Everard, A., Belzer, C., Geurts, L., Ouwerkerk, J. P., Druart, C., Bindels, L. B., et al. (2013) Cross-talk between Akkermansia muciniphila and intestinal epithelium controls diet-induced obesity. *Proc. Natl. Acad. Sci. U. S. A.* **110**, 9066–9071
- Depommier, C., Vitale, R. M., Iannotti, F. A., Silvestri, C., Flament, N., Druart, C., et al. (2021) Beneficial effects of Akkermansia muciniphila are not associated with major changes in the circulating endocannabinoidome but linked to higher monopalmitoyl-glycerol levels as new PPAR α agonists. *Cells* **10**, 185
- Bae, M., Cassilly, C. D., Liu, X., Park, S. M., Tusi, B. K., Chen, X., et al. (2022) Akkermansia muciniphila phospholipid induces homeostatic immune responses. *Nature* **608**, 168–173
- Pujo, J., Petitfils, C., Le Faouder, P., Eeckhaut, V., Payros, G., Maurel, S., et al. (2021) Bacteria-derived long chain fatty acid exhibits anti-inflammatory properties in colitis. *Gut* **70**, 1088–1097
- Le Roy, T., Van der Smissen, P., Paquot, A., Delzenne, N., Muccioli, G. G., Collet, J. F., and Cani, P. D. (2020) Dysosmobacter welbionis gen. nov., sp. nov., isolated from human faeces and emended description of the genus Oscillibacter. *Int. J. Syst. Evol. Microbiol.* **70**, 4851–4858
- Le Roy, T., Moens de Hase, E., Van Hul, M., Paquot, A., Pelicaen, R., Régnier, M., et al. (2022) Dysosmobacter welbionis is a newly isolated human commensal bacterium preventing diet-induced obesity and metabolic disorders in mice. *Gut* **71**, 534–543
- Guillemot-Legrès, O., Mutemberezi, V., Buisseret, B., Paquot, A., Palmieri, V., Bottemanne, P., et al. (2019) Colitis alters oxysterol metabolism and is affected by 4 β -hydroxycholesterol administration. *J. Crohns Colitis* **13**, 218–229
- Le Faouder, P., Baillif, V., Spreadbury, I., Motta, J. P., Rousset, P., Chêne, G., et al. (2013) LC-MS/MS method for rapid and concomitant quantification of pro-inflammatory and pro-resolving polyunsaturated fatty acid metabolites. *J. Chromatogr. B Analyt. Technol. Biomed. Life Sci.* **932**, 123–133
- Alhouayek, M., Lambert, D. M., Delzenne, N. M., Cani, P. D., and Muccioli, G. G. (2011) Increasing endogenous 2-arachidonoylglycerol levels counteracts colitis and related systemic inflammation. *FASEB J.* **25**, 2711–2721
- Lynes, M. D., Leiria, L. O., Lundh, M., Bartelt, A., Shamsi, F., Huang, T. L., et al. (2017) The cold-induced lipokine 12,13-diHOME promotes fatty acid transport into brown adipose tissue. *Nat. Med.* **23**, 631–637
- Stanford, K. I., Lynes, M. D., Takahashi, H., Baer, L. A., Arts, P. J., May, F. J., et al. (2018) 12,13-diHOME: an exercise-induced lipokine that increases skeletal muscle fatty acid uptake. *Cell Metab.* **27**, 1111–1120.e3
- Macedo, A. P. A., Muñoz, V. R., Cintra, D. E., and Pauli, J. R. (2022) 12,13-diHOME as a new therapeutic target for metabolic diseases. *Life Sci.* **290**, 120229
- Zhao, X., Zhang, Y., Strong, R., Grotta, J. C., and Aronowski, J. (2006) 15d-Prostaglandin J2 activates peroxisome proliferator-activated receptor-gamma, promotes expression of catalase, and reduces inflammation, behavioral dysfunction, and neuronal loss after intracerebral hemorrhage in rats. *J. Cereb. Blood Flow Metab.* **26**, 811–820
- Li, J., Guo, C., and Wu, J. (2019) 15-Deoxy- Δ -(12,14)-Prostaglandin J2 (15d-PGJ2), an endogenous ligand of PPAR-gamma: Function and mechanism. *PPAR Res.* **2019**, 7242030
- Bargut, T. C., Aguila, M. B., and Mandarin-de-Lacerda, C. A. (2016) Brown adipose tissue: updates in cellular and molecular biology. *Tissue Cell* **48**, 452–460
- Ogawa, N., Sugiyama, T., Morita, M., Suganuma, Y., and Kobayashi, Y. (2017) Total synthesis of resolvin D5. *J. Org. Chem.* **82**, 2032–2039
- Chiang, N., Fredman, G., Bäckhed, F., Oh, S. F., Vickery, T., Schmidt, B. A., and Serhan, C. N. (2012) Infection regulates pro-resolving mediators that lower antibiotic requirements. *Nature* **484**, 524–528
- Gobbetti, T., Dalli, J., Colas, R. A., Federici Canova, D., Aursnes, M., Bonnet, D., et al. (2017) Protectin DI(n-3 DPA) and resolvin D5(n-3 DPA) are effectors of intestinal protection. *Proc. Natl. Acad. Sci. U. S. A.* **114**, 3963–3968
- Takagi, T., Naito, Y., Mizushima, K., Hirai, Y., Kamada, K., Uchiyama, K., et al. (2019) 15-Deoxy-Delta(12,14)-prostaglandin J2 ameliorates dextran sulfate sodium-induced colitis in mice through heme oxygenase-1 induction. *Arch. Biochem. Biophys.* **677**, 108183
- Kim, W., Jang, J. H., Zhong, X., Seo, H., and Surh, Y. J. (2021) 15-Deoxy- big up tri, open(12,14)-prostaglandin J2 promotes resolution of experimentally induced colitis. *Front. Immunol.* **12**, 615803
- Neuhofer, A., Zeyda, M., Mascher, D., Itariu, B. K., Murano, L., Leitner, L., et al. (2013) Impaired local production of proresolving lipid mediators in obesity and 17-HDHA as a potential treatment for obesity-associated inflammation. *Diabetes* **62**, 1945–1956
- Luo, J., Hu, S., Fu, M., Luo, L., Li, Y., Li, W., et al. (2021) Inhibition of soluble epoxide hydrolase alleviates insulin resistance and hypertension via downregulation of SGLT2 in the mouse kidney. *J. Biol. Chem.* **296**, 100667
- Zhang, J., Yang, C., Qiu, H., Yang, J., Wu, K., Ding, S., et al. (2022) 14,15-EET involved in the development of diabetic cardiac hypertrophy mediated by PPARs. *Prostaglandins Other Lipid Mediat.* **159**, 106620
- Yang, T., Peng, R., Guo, Y., Shen, L., Zhao, S., and Xu, D. (2013) The role of 14,15-dihydroxyeicosatrienoic acid levels in inflammation and its relationship to lipoproteins. *Lipids Health Dis.* **12**, 151
- Dai, N., Yang, C., Fan, Q., Wang, M., Liu, X., Zhao, H., and Zhao, C. (2020) The anti-inflammatory effect of soluble epoxide hydrolase inhibitor and 14, 15-EET in Kawasaki disease through PPARgamma/STAT1 signaling pathway. *Front. Pediatr.* **8**, 451
- Abot, A., Wemelle, E., Laurens, C., Paquot, A., Pomie, N., Carper, D., et al. (2021) Identification of new enterosynes using prebiotics: roles of bioactive lipids and mu-opioid receptor signalling in humans and mice. *Gut* **70**, 1078–1087
- Vangaveti, V., Baune, B. T., and Kennedy, R. L. (2010) Hydroxyoctadecadienoic acids: novel regulators of macrophage differentiation and atherogenesis. *Ther. Adv. Endocrinol. Metab.* **1**, 51–60
- Dandona, P., Mohanty, P., Ghanim, H., Aljada, A., Browne, R., Hamouda, W., et al. (2001) The suppressive effect of dietary restriction and weight loss in the obese on the generation of reactive oxygen species by leukocytes, lipid peroxidation, and protein carbonylation. *J. Clin. Endocrinol. Metab.* **86**, 355–362
- Jira, W., Spiteller, G., Carson, W., and Schramm, A. (1998) Strong increase in hydroxy fatty acids derived from linoleic acid in human low density lipoproteins of atherosclerotic patients. *Chem. Phys. Lipids* **91**, 1–11

37. Perez-Berezo, T., Pujo, J., Martin, P., Le Faouder, P., Galano, J. M., Guy, A., *et al.* (2017) Identification of an analgesic lipopeptide produced by the probiotic *Escherichia coli* strain Nissle 1917. *Nat. Commun.* **8**, 1314
38. Trico, D., Di Sessa, A., Caprio, S., Chalasani, N., Liu, W., Liang, T., *et al.* (2019) Oxidized derivatives of linoleic acid in pediatric metabolic syndrome: is their pathogenic role modulated by the genetic background and the gut microbiota? *Antioxid. Redox Signal.* **30**, 241–250
39. Altmann, R., Hausmann, M., Spöttl, T., Gruber, M., Bull, A. W., Menzel, K., *et al.* (2007) 13-Oxo-ODE is an endogenous ligand for PPARgamma in human colonic epithelial cells. *Biochem. Pharmacol.* **74**, 612–622
40. Umeno, A., Shichiri, M., Ishida, N., Hashimoto, Y., Abe, K., Kataoka, M., *et al.* (2013) Singlet oxygen induced products of linoleates, 10- and 12-(Z,E)-hydroxyoctadecadienoic acids (HODE), can be potential biomarkers for early detection of type 2 diabetes. *PLoS One* **8**, e63542
41. Mikkelsen, R. B., Arora, T., Trošt, K., Dmytriyeva, O., Jensen, S. K., Meijnikman, A. S., *et al.* (2022) Type 2 diabetes is associated with increased circulating levels of 3-hydroxydecanoate activating GPR84 and neutrophil migration. *iScience* **25**, 105683
42. Al-Sulaiti, H., Diboun, I., Agha, M. V., Mohamed, F. F. S., Atkin, S., Dömling, A. S., *et al.* (2019) Metabolic signature of obesity-associated insulin resistance and type 2 diabetes. *J. Transl. Med.* **17**, 348
43. Hosseinkhani, S., Salari, P., Bandarian, F., Asadi, M., Shirani, S., Najjar, N., *et al.* (2022) Circulating amino acids and acylcarnitines correlated with different CAC score ranges in diabetic postmenopausal women using LC-MS/MS based metabolomics approach. *BMC Endocr. Disord.* **22**, 186
44. Adebayo, A. S., Roman, M., Zakkar, M., Yusoff, S., Gulston, M., Joel-David, L., *et al.* (2022) Gene and metabolite expression dependence on body mass index in human myocardium. *Sci. Rep.* **12**, 1425
45. Zhao, H., Chen, J., Chai, J., Zhang, Y., Yu, C., Pan, Z., *et al.* (2017) Cytochrome P450 (CYP) epoxygenases as potential targets in the management of impaired diabetic wound healing. *Lab. Invest.* **97**, 782–791
46. Gilroy, D., Colville-Nash, P., Willis, D., Chivers, J., Paul-Clark, M. J., and Willoughby, D. A. (1999) Inducible cyclooxygenase may have anti-inflammatory properties. *Nat. Med.* **5**, 698–701
47. Morisseau, C., Inceoglu, B., Schmelzer, K., Tsai, H. J., Jinks, S. L., Hegedus, C. M., and Hammock, B. D. (2010) Naturally occurring monoepoxides of eicosapentaenoic acid and docosahexaenoic acid are bioactive antihyperalgesic lipids. *J. Lipid Res.* **51**, 3481–3490
48. Anita, N. Z., Forkan, N., Kamal, R., Nguyen, M. M., Yu, D., Major-Orfao, C., *et al.* (2021) Serum soluble epoxide hydrolase related oxylipins and major depression in patients with type 2 diabetes. *Psychoneuroendocrinology* **126**, 105149
49. Chun, H. W., Lee, J., Pham, T. H., Lee, J., Yoon, J. H., Lee, J., *et al.* (2020) Resolvin D5, a lipid mediator, inhibits production of interleukin-6 and CCL5 via the ERK-NF-kappaB signaling pathway in lipopolysaccharide-stimulated THP-1 cells. *J. Microbiol. Biotechnol.* **30**, 85–92
50. Morgenstern, J., Fleming, T., Kadiyska, I., Brings, S., Groener, J. B., Nawroth, P., *et al.* (2018) Sensitive mass spectrometric assay for determination of 15-deoxy-Delta(12,14)-prostaglandin J(2) and its application in human plasma samples of patients with diabetes. *Anal. Bioanal. Chem.* **410**, 521–528
51. Alhouayek, M., Buisseret, B., Paquot, A., Guillemot-Legris, O., and Muccioli, G. G. (2018) The endogenous bioactive lipid prostaglandin D(2)-glycerol ester reduces murine colitis via DPL and PPARgamma receptors. *FASEB J.* **32**, 5000–5011